



The Open Civil Engineering Journal

Content list available at: www.benthamopen.com/TOCIEJ/

DOI: 10.2174/1874149501711010001



RESEARCH ARTICLE

Study on Cross-shaped Concrete Filled Steel Tubular Stub Columns Subjected to Axial Compression: Experiments and Design Method

Chen Qiguang¹, Cai Jian^{1,2}, Zuo ZhiLiang^{1,*}, Huang Jinxuan¹ and Wei Jieying¹¹School of Civil Engineering and Transportation, South China University of Technology, Guangzhou 510641, P. R. China²State Key Laboratory of Subtropical Building Science, South China University of Technology, Guangzhou 510641, P. R. China

Received: January 21, 2016

Revised: October 04, 2016

Accepted: October 07, 2016

Abstract: Despite its wide application prospect, researches on the cross-shaped concrete filled steel tubular (CFT) columns are scarce, and no design method can be used. This paper concerns with the axial load behavior of cross-shaped CFT stub columns. Five specimens were tested to examine the influences of three parameters on the characteristics of failure, the bearing capacity and deformability. The parameters include the width-thickness ratios of steel plates, the yield strengths of steel and the sectional dimensions. Experimental results demonstrate that the global outward bulge of steel tube near the concave corners is significant, so that the stresses on the steel tube distribute unevenly and the confinement effects on the concrete are inferior to the rectangular CFT columns. By decreasing the width-thickness ratio of each steel plate, the global outward bulge near the concave corners was smaller, but the ductility could be improved only when it decreased by 2.08 times. By increasing the yield strength of steel to 1.47 times, the bearing capacity and deformation were inversely smaller, but the ductility was increased. By increasing the length-width ratio of each leg to 2.25 times, the global outward bulge was increased and local buckling occurred earlier. Then the application scopes for evaluating the maximum strength of specimens by the methods in design codes are provided. A new method is also proposed by considering the confinement effects of concrete and the strength loss of steel tube. The results predicted by the proposed method show good agreement with the experimental ones.

Keywords: Axial compression, Cross-shaped CFT, Design methods, Experiments, Global outward bulge, Stub column.

1. INTRODUCTION

Concrete-filled steel tubular (CFT) columns have been widely used as structural members. Extensive investigations have been carried out to study the mechanical performance of circular, square and rectangular CFT columns [1 - 5], and several researches focused on the special-shaped CFT columns, such as the T-shaped, L-shaped and elliptic CFT columns [6 - 11], while the studies on other kinds of special-shaped CFT columns were scarce, such as the cross-shaped CFT columns [12 - 16]. The study results show that the mechanical behavior of special-shaped CFT columns with flat steel plates or concave corners, such as the L-shaped, T-shaped and cross-shaped CFT columns, is inferior to that of circular CFT columns. It is because that the flexural stiffness around the middle area of each steel plate of a special-shaped CFT column is weaker to resist the outward extrusion of core concrete, like the case of square and rectangular CFT columns. Especially, the length of several steel plates of the T-shaped and L-shaped CFT columns is larger than the others, so failure always occurs around these areas. What is worse, for the special-shaped CFT columns with concave corners, the steel tube near these concave corners bulges entirely outward, because the transverse resultant force of the two steel plates next to the concave corners is directed outward under the outward extrusion of concrete. It results in a further loss of bearing capacity and deformability. On the aggregate, if the width-thickness ratios of steel

* Address correspondence to this author at the School of Civil Engineering and Transportation, South China University of Technology, Guangzhou 510640, P.R. China; Tel: +86 20 87114801; Fax: +86 20 87114801; E-mail: ctzlzuo@scut.edu.cn

plates are the same, the total confinement effects on core concrete of the special-shaped CFT columns are remarkably smaller than those of the circular CFT columns, and the stresses of special-shaped steel tube distribute unevenly, especially for the CFT columns with concave corners.

However, special-shaped CFT columns, mainly the L-shaped, T-shaped and cross-shaped CFT columns, have been extensively used in engineering structures in recent years [17], on account of their convenient construction at beam–column joints, larger moment of inertia of cross-section, and improved agreement with the design need of the architectural schemes. Especially, there are two symmetrical axes in a general cross-shaped section, so compared with the L-shaped and T-shaped CFT columns, the mechanical behaviors of the cross-shaped CFT columns in different loading directions under cyclic load are more uniform. Only a few of researches on the mechanical performances of cross-shaped CFT columns have been conducted. Based on the nonlinear analysis method, Cao [12] studied the influences, load angle, axial compression ratio, steel ratio and yield strength of steel tube, on the curvature ductility coefficient of cross-shaped CFT columns under biaxial bending and compression. A type of cross-shaped CFT column composed of square CFT columns is proposed by Chen [13], as shown in Fig. (1), and the calculation method and mechanical property of slender specimens were studied by the superposition theory, finite element analysis and axial compression experiment.

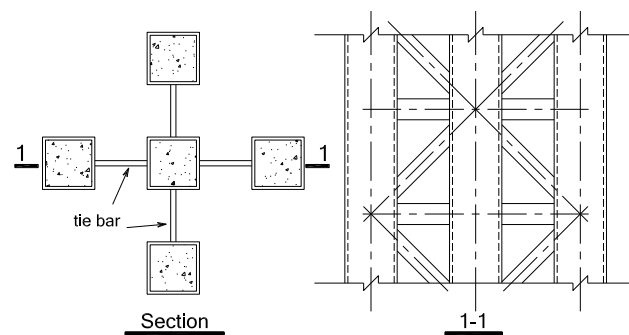


Fig. (1). The composite cross-shaped section [13].

Despite its wide application prospect, researches on the cross-shaped CFT columns are scarce, and no design code provides design guidelines of these members that can be used in engineering projects. In this paper, experimental investigations conducted on five normal cross-shaped CFT columns subjected to axial compression, are reported. The primary parameters considered in this test program are: (1) maximum width-thickness ratios of steel plates ($\alpha_1 \sqrt{f_{ys} / 235} / t$); (2) yield strengths of steel (f_{ys}); (3) sectional dimensions ($k = a_1 / b_1$ or b_2 / a_2). These factors were experimentally investigated to assess their influences on the characteristics of failure, the bearing capacity and deformability, and the stress distribution on the steel tube. Then, through comparing the results predicted by the methods in the design codes (ACI [19], EC4 [20], GJB [21] and DBJ [22]) with the experimental results, the scopes of application about the parameters for each method, such as the limits of the maximum width-thickness ratio of steel plates and the relevant steel strength, are suggested. These methods are optional methods to predict the strength of cross-shaped CFT stub column, but the application scopes are small. Finally, to establish a method with wider applicability, by considering the confinement effects of concrete and strength loss of steel tube, a theoretical method is proposed and verified by the test results.

2. EXPERIMENTAL PROGRAM

Five 1:3 scale cross-shaped CFT stub columns designated as the specimens C1~C5 were tested. The details of the specimens are shown in Table 1 and Fig. (2). The maximum width-thickness ratios ($\alpha_1 \sqrt{f_{ys} / 235} / t$) range from 11 to 39. The yield strengths (f_{ys}) range from 239MPa to 348MPa. The values of a_1 / b_1 and b_2 / a_2 are both equal to 1 for the specimens C1-C4, while they are equal to 2.25 for the specimen C5. Namely, the sections of all specimens are symmetrical around two axes. The initial clear height is 720mm for the specimens C1-C4, while it is 1320mm for the specimen C5. The steel tubes were fabricated by welding twelve steel plates together. Based on the study results of Uy [23], if the width-thickness ratio of heavily welded steel plate is smaller than the yield width-thickness ratio limit which is about 65, the ultimate strength is not affected by the residual stresses. Besides, the test results in this paper showed that the local buckling occurred after the peak load for all the specimens. Therefore, in this study, it is assumed that the

ultimate strength is not significantly affected by the residual stresses due to welding. The characteristic 28-day cubic compressive strength of concrete ($f_{cu,k}$) for all the specimens is 54.7MPa.

Table 1. Details of the specimens and experimental results.

No.	$a_1/a_2/b_1/b_2/t$	f_{ck}/f_{ys}	$a_1\sqrt{f_{ys}/23.5}/t$	$\epsilon_b/\epsilon_u/\epsilon_{85}/\times 10^{-6}$	DI	N_b	N_u	$\frac{N_u}{N_{un}}$	$\frac{N_b}{N_{un}}$
	(mm)	(MPa)				(kN)	(kN)		
C1	80/ 80/ 80/ 80/ 3.64	41.58/ 348	27	(9579)/ 3486/ 5472	1.57	(1520)	2064	0.89	(0.66)
C2	80/ 80/ 80/ 80/ 5.6	41.58/ 346	17	—/ 5532/ 7936	1.43	—	2754	0.96	—
C3	80/ 80/ 80/ 80/ 7.74	41.58/ 261	11	—/ 5747/ 33830	5.89	—	3326	1.17	—
C4	80/ 80/ 80/ 80/ 3.72	41.58/ 239	22	(11883)/ 3692/ 4772	1.29	(1410)	2155	1.10	(0.72)
C5	180/ 80/ 180/ 80/ 5.6	41.58/ 346	39	(5647)/ 2842/ 6406	2.25	(3633)	4096	0.75	(0.67)

Notes: 1. a_1, a_2, b_1, b_2 —the width of each side, as shown in Fig. (2). 2. t —the thickness of steel tube. 3. f_{ys}, f_{ck} —the yield strength of steel and the characteristic compressive strength of concrete prism, calculated by $f_{ck}=0.76 f_{cu,k}$. 4. N_b, ϵ_b —the load and corresponding average longitudinal strain when the local buckling occurred, it means the local buckling appeared at the post-peak stage when they are marked by “()”, and when local buckling was not found, they are marked by “—”. 5. N_u, ϵ_u —the experimental maximum load and corresponding average longitudinal strain. 6. ϵ_{85} —the average longitudinal strain when the load falls to 85% of the maximum load. 7. N_{un} —the nominal strength of the specimens, $N_{un}=f_{ck}A_c+f_{ys}A_s$, where A_c is the area of concrete, A_s is the area of steel tube. 8. DI— ductility index, defined as $DI=0.75\times(\epsilon_{85}/\epsilon_{75})$ [18], where ϵ_{75} is the average longitudinal strain when the load reaches 75% of the maximum load in the pre-peak stage.

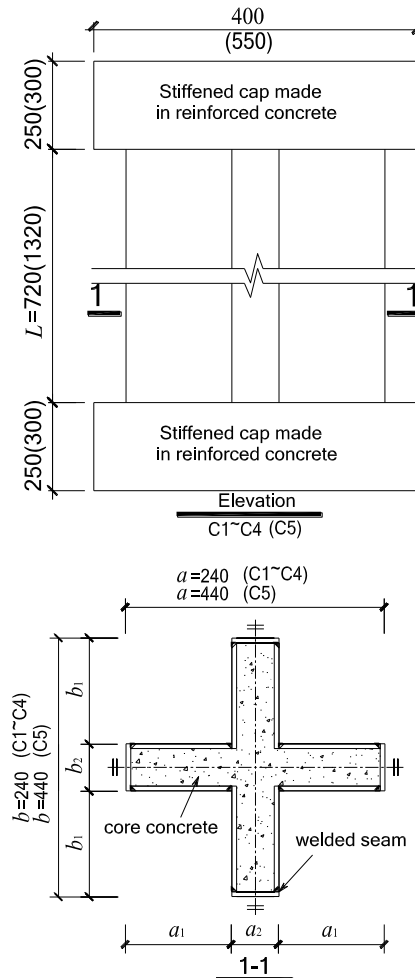


Fig. (2). Details of the specimens.

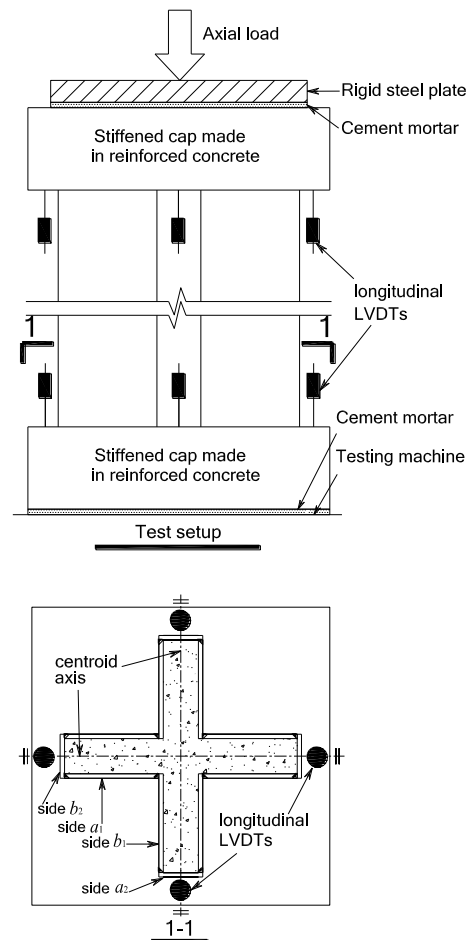


Fig. (3). Test setup.

A 15000kN universal testing machine was employed to carry out the test, and the loading position was the centroid point of cross-shaped section, as shown in Fig. (3). Four pairs of linear variable displacement transducers (LVDTs) were arranged longitudinally between the two caps to measure the axial shortening of four symmetrical positions along the centroid axes, respectively. The average longitudinal strain (ϵ) can be calculated by dividing the average displacement difference, obtained from four pairs of LVDTs, by the initial clear height of specimen (L). The wire strain gauges were arranged on the steel tube near the mid-height to measure the transverse and longitudinal strains of the steel plates.

The specimens were loaded by monotonically increasing vertical displacement at a rate of 0.2mm/min. The global outward bulge and local buckling of steel tube were observed during the test. The loads when local buckling occurred were recorded. Testing was terminated when the longitudinal deformation became excessively large and the outward bulge of steel tube was obvious.

3. EXPERIMENTAL RESULTS AND DISCUSSIONS

The experimental results are shown and discussed in this section, such as the experimental phenomena and failure modes, characteristics of load bearing and deformability, and the strain of steel plate.

3.1. Experimental Phenomena and Failure Modes

The typical failure modes of specimens were local buckling of steel plates and global outward bulge of steel tube at the concave corners near the mid-height of the column, as shown in Fig. (4). The maximum width-thickness ratios of steel plates of the specimens C1, C4 and C5 ($a_1 \sqrt{f_{ys} / 235} / t = 27, 22$ and 39 , respectively) are relatively large among the specimens. The failure modes of them were similar. When reaching the maximum load, global outward bulge of steel tube at the concave corners were found. At the load descending stage, local buckling appeared randomly on the

steel plates with relative larger width-thickness ratio, such as the side- a_1 steel plate and the side- b_1 steel plate. Global outward bulge of steel tube at the concave corners were more obvious at the late loading stage, and each leg of the cross-shaped steel tube deformed similarly as a single column which was subjected to eccentric compression. The failure modes of specimens C2 and C3, whose $a_1\sqrt{f_{ys}/235}/t$ are relatively small among the specimens, were similar with those of the specimens C1, C4 and C5, but the globe outward bulge at the concave corners was smaller, and no local buckling of steel plate was found till the end.

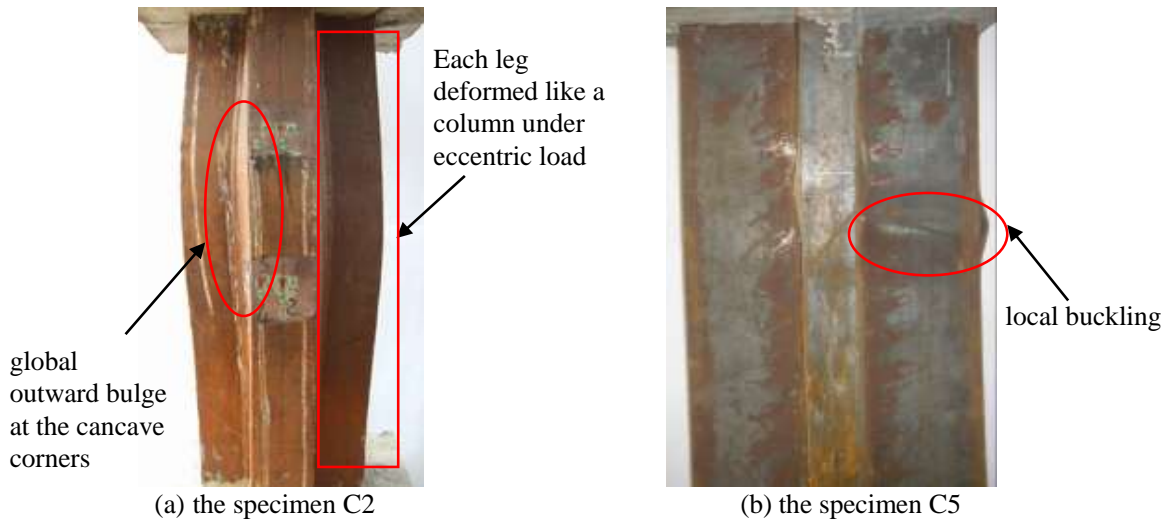


Fig. (4). Typical failure modes.

The experimental phenomena indicate that the width-thickness ratio of steel plate is a key factor affecting the failure modes of a cross-shaped CFT stub column. On the other hand, as distinguished from the CFT columns without concave corners, the global outward bulge of the steel tube at the concave corners of the cross-shaped CFT columns has significant influences on the mechanical behavior. Besides, increasing the yield strength of steel has little effect on the failure modes.

3.2. Characteristics of Load Bearing and Deformability

The curves of load (N) versus average longitudinal strain (ϵ) of all specimens are shown in Fig. (5). The loads corresponding to the initiation of local buckling (N_b) are marked on the curves, designated as B1 to B5, where the points B2 and B3 are absent because local buckling was not found for the specimens C2 and C3. Table 1 lists the key results on the curves, including the experimental maximum loads and corresponding average longitudinal strains (N_u and ϵ_u), the loads and corresponding average longitudinal strains at the points B (N_b and ϵ_b), the ratios N_u/N_{un} and N_b/N_{un} , and the ductility indexes $DI=0.75\times(\epsilon_{85}/\epsilon_{75})$ [18]. As shown in Fig. (5) and Table 1, the characteristics of load bearing and deformability of the specimens are as follows.

1. The maximum loads (N_u) of the specimens C3 and C4 are larger than their nominal strengths (N_{un}), $N_u/N_{un}\geq 1$, respectively. The so-called nominal strength, $N_{un}=f_{ck}A_c+f_{ys}A_s$, is the theoretical maximum strength of a CFT column in a case that the average stresses of the concrete and the steel tube are f_{ck} and f_{ys} , respectively. When the parameters relevant to the longitudinal strength of specimens, such as the thickness and strength of steel tube, are changed, it is more meaningful to investigate the load bearing characteristics by the ratio N/N_{un} than by the practical load (N) directly. Essentially, when other parameters are the same, there are three factors affecting the ratio of a practical load (N) and the nominal strength (N_{un}), such as the N_u/N_{un} and the N_{85}/N_{un} , where N_{85} refers to the load when it falls to 85% of the maximum load. Besides, they also affect the value of deformation in these conditions, such as the ϵ_u and ϵ_{85} . Take the ratio N_u/N_{un} for example, firstly, by increasing the confinement effects of the steel tube on the core concrete, the mean strength and the elastoplastic deformation capacity of core concrete are larger than the plain concrete, then the ratio N/N_{un} is increased, and the average longitudinal strain (ϵ_u) is increased too. Second, if the stresses of steel tube distribute more uniformly due to a smaller extent of outward bulge, more area of steel tube can reach yield at the peak load, then the ratio N_u/N_{un} is increased. It also

contributes to a larger deformation (ϵ_u), because the plastic deformation capacity of the integral steel tube section is increased. Third, when the total strength of steel tube which contributes to the bearing capacity of the column is smaller, the ratio N_u/N_{un} and the relevant deformation (ϵ_u) are increased. It is because that the strength loss of steel tube caused by a same extent of outward bulge or local buckling is smaller. However, if the extent of outward bulge is effectively reduced and meanwhile the total strength of steel tube is increased, for instance, by increasing the thickness of steel tube, the ratio N_u/N_{un} is also enhanced. For other loading stage, these three factors also influence the ratio N/N_{un} and the relevant deformation (ϵ), only the extent of impact of each factor changes.

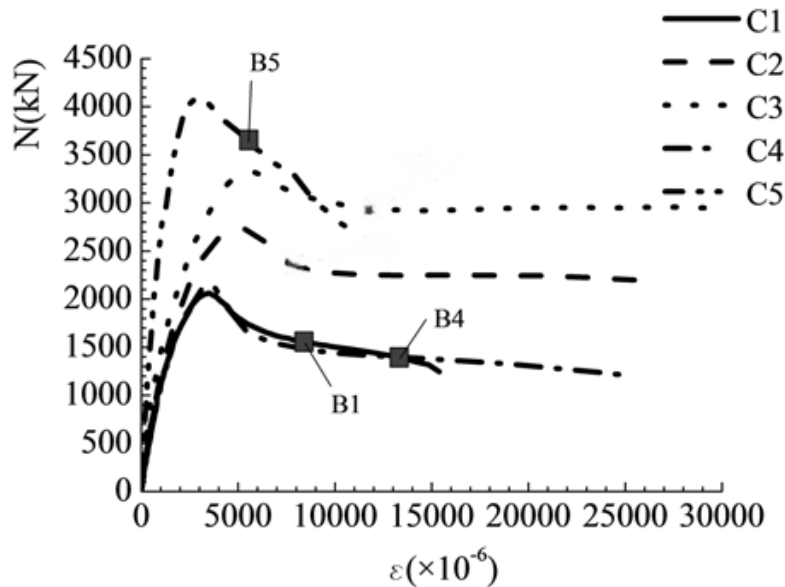


Fig. (5). Load (N) - average longitudinal strain (ϵ) curves.

For the specimen C3, the width-thickness ratio of the side- α_1 steel plate is the smallest of all specimens, and from the experiment, the outward bulge of steel tube is also the smallest. It gives rise to the largest confinement effects on the core concrete, and the longitudinal stresses of almost the whole steel tube can reach yield at the peak load, as discussed later. As a result, the ratio N_u/N_{un} reaches 1.17. For the specimen C4, the yield strength of steel is only 239MPa and its thickness of steel tube is relatively small ($t=3.72\text{mm}$), so the total strength of steel tube which contributes to the bearing capacity of the column is the smallest of all specimens. Besides, part of the core concrete near the convex corners is constrained. Both the cases above are beneficial to the increase of ratio N_u/N_{un} , and the beneficial effects are larger than the adverse effects due to a relatively small t . As a result, for the specimen C4, the ratio N_u/N_{un} reaches 1.1. For the specimens C1, C2 and C5, the steel tubes have larger contribution to the cross section bearing capacity than the case of specimen C4, and the outward bulge of steel tubes is larger than the case of specimen C3 because the width-thickness ratios of steel tubes are larger. As a result, the ratios N_u/N_{un} are all smaller than 1.0. Especially, for the specimen C5, the width-thickness ratio of the side- α_1 steel plate is the largest. The ratio N_u/N_{un} of it is only 0.75 on account of large outward bulge of steel tube.

2. The parameters of specimens C1 and C2 are nearly the same except for the thickness of steel tube, $t_{C2}/t_{C1}=1.54$. The situation is similar between the specimens C3 and C4, $t_{C3}/t_{C4}=2.08$. As shown in Fig. (5), with the increase of t , namely, the decrease of width-thickness ratio of each steel plate, the initial axial rigidity is larger, and the strength-descending rate after the peak load is generally smaller. There is an increase of the ratio N_u/N_{un} by 8% and an increase of the relevant ϵ_u by 59%, compared the specimen C2 with the specimen C1, as shown in Table 1. And, they are 6% and 56%, respectively, compared the specimen C3 with the specimen C4. In fact, by increasing t , the flexural stiffness for resisting outward bulge of steel tube is increased, so that the outward bulge of steel tube, especially the areas near the mid-width of each steel plate and the areas near the concave corners, is smaller. As a result, the confinement effects of steel tube on the core concrete are improved. Besides, the stresses on the steel tube distribute more uniformly, so that the relevant total axial strength of the steel tube is increased. These two effects lead to the increases of ratio N_u/N_{un} and the relevant ϵ_u . Furthermore, although the

difference of thickness between the specimens C3 and C4 (t_{C3}/t_{C4}) is larger than that of the specimens C2 and C1 (t_{C2}/t_{C1}), the increasing rates of N_u/N_{un} and ε_u between the specimens C3 and C4 are merely approximative to those between the specimens C2 and C1. The reason is, as discussed before, the total strength of steel tube of the specimen C4 which contributes to the bearing capacity of the column is the smallest of all specimens, so that the ratio N_u/N_{un} and ε_u of the specimen C4 are both relatively large and more closer to those of the specimen C3. In addition, the ε_{85} of the specimen C2 is 1.45 times that of the specimen C1, and it is 7.09 times compared the specimen C3 with the specimen C4. It indicates that the load resistant capacity at the post-peak stage is increased by increasing t . Furthermore, as distinguished from the ε_u , the increasing rates of ε_{85} are considerably different for the specimens with varied yield strength of steel and varied increasing rate of t . As it can be seen, the increasing rate of ε_{85} is smaller than that of ε_u , compared the specimen C2 with the specimen C1, $t_{C2}/t_{C1}=1.54$. But, it is significantly larger than that of ε_u , compared the specimen C3 with the specimen C4, $t_{C3}/t_{C4}=2.08$. It is because the trend of outward extrusion of core concrete and the trend of outward bulge of steel tube in the post-peak stage are extremely larger than those in the pre-peak stage. In the post-peak stage, it has a larger demand on the flexural stiffness of steel tube for resisting outward bulge and preventing large strength loss. Besides, with larger yield strength of steel, the strength loss of the specimen C2 caused by outward bulge of steel tube in the post-peak stage is larger, so that the increasing rate of ε_{85} compared with the specimens C2 and C1 should be smaller. Similarly, although the indexes ε_u and ε_{85} that reflected the deformability are both increased by increasing t , another index, the ductility index DI , does not change in the same way. The DI , which is essentially the ratio of ε_{85} and ε_{75} , is increased by 4.57 times compared the specimen C3 with the specimen C4, but it is 0.91 times compared the specimen C2 with the specimen C1. It means that the ductility can only be increased in case that the increasing rate of t is large enough. It is because that the increasing rates of ε_{75} and ε_u by increasing t are approximative according to the experimental data, but the increasing rate of ε_{85} only becomes larger than that of ε_u by increasing a large amount of t , such as the case between the specimens C3 and C4.

3. The difference between the specimens C2 and C5 is the sectional dimension ($k=\alpha_1/b_2=b_1/a_2$). As shown in Table 1, for the specimen C5 ($k=2.25$), the ratio N_u/N_{un} that is related to the confinement effects of concrete and axial strength of steel tube, and the values of ε_u , ε_{85} and DI that are related to the deformability, are all smaller than those of the specimen C2 ($k=1$). It is because that the width-thickness ratios of the steel plates on the side- α_1 and side- b_1 increase by increasing k . Besides, the strain that local buckling of the specimen C5 appeared (ε_b) is the smallest of all specimens.
4. The parameters between the specimens C1 and C4 are similar except that the yield strength of steel (f_{ys}) of the specimen C1 is 1.46 times that of the specimen C4. As shown in Fig. (5), no influence on the initial axial rigidity of specimen can be found by varying the f_{ys} . As shown in Table 1, the values of N_u , N_u/N_{un} , ε_u , ε_{85} , and DI of the specimen C1 are 0.96, 0.81, 0.94, 1.15 and 1.22 times those of the specimen C4, respectively. By increasing f_{ys} , the transverse stresses of steel tube become larger at the peak load. It is beneficial to increase the confinement effects on core concrete. As a result, logically, it seems that the values of N_u , N_u/N_{un} , ε_u , ε_{85} , and DI should all become larger. However, other situations should be considered. First, increasing f_{ys} has no influence on the flexural stiffness of steel plate. It means that, for the specimens C1 and C4, the extent of outward bulge of steel tube and the relevant stress distribution pattern should be similar. Second, by increasing f_{ys} , the strength loss of steel tube caused by a same extent of outward bulge should be larger, because the axial strength of steel tube that contributes to the cross section bearing capacity becomes larger. Synthesize the adverse effect on the strength loss of steel tube and the beneficial effect on constraining the concrete, by increasing f_{ys} in a certain amount, such as that in this experiment, the values of N_u , N_u/N_{un} and ε_u may inversely become smaller. In addition, the outward extrusive deformation of concrete in the post-peak stage is larger. So, in the post-peak stage, the steel tube with a larger f_{ys} can provide larger transverse stresses to constrain the concrete than those in the pre-peak stage. Then, by increasing f_{ys} , the indexes ε_{85} and DI related to the load resistant capacity in the post-peak stage may become larger.

3.3. Strain of Steel Plate

The width-thickness ratio of the side- α_1 steel plate in the specimen C5 is the largest of all the specimens. As a typical example, the strain distribution characteristic on the side- α_1 steel plate in the middle height of the specimen C5 are investigated. The positions of wire strain gauges are shown in Fig. (6). The curves of normalized loads (N/N_u) versus

longitudinal strains (ϵ_L) and transverse strains (ϵ_H) on the side- α_1 steel plate of the specimen C5 are shown in Fig. (7) and Fig. (8).

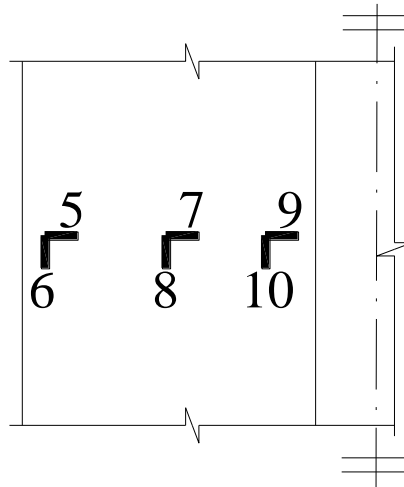


Fig. (6). Positions of strain gauges of the specimen C5.

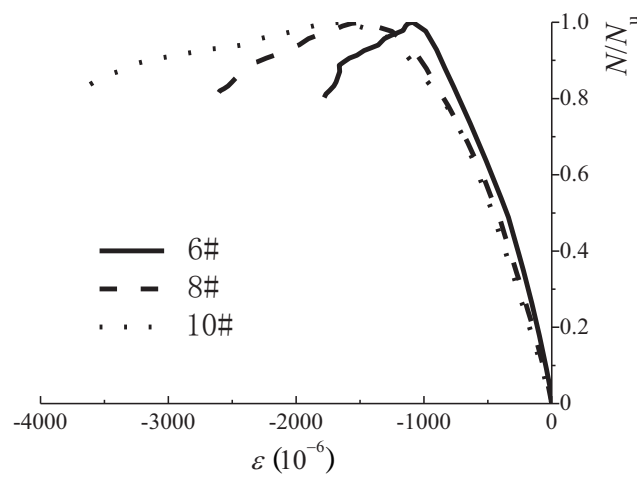


Fig. (7). N/N_u - ϵ_L relationship curves of the specimen C5.

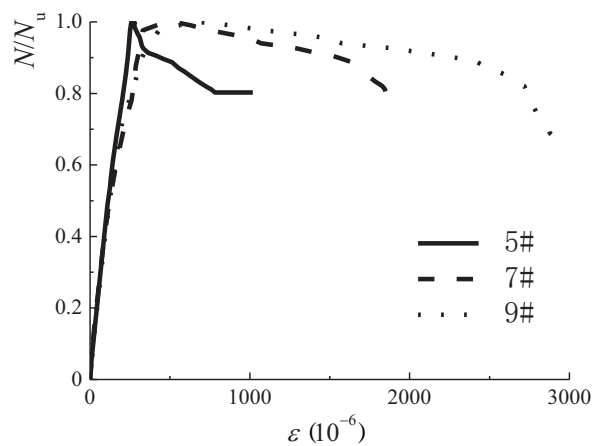


Fig. (8). N/N_u - ϵ_H relationship curves of the specimen C5.

The average longitudinal strains (ε) of all specimens, achieved from the readings on LVTDs, have reached yield at the peak load, as shown in Fig. (5). However, not all the longitudinal strains on the steel plate, achieved from the readings on strain gauges, can reach yield, as shown in Fig. (7). Besides, the compressive strains increase from the convex corner to the concave corner given by 6#<8#<10#. It is because that the areas near the concave corners tend to bulge outward integrally under the outward extrusion of core concrete. It makes each leg of the cross-shaped steel tube deform similarly as a single column subjected to eccentric compression, and the global outward bulge near the convex corner of each leg is the largest, as shown in Fig. (4). As a result, the longitudinal strains of steel tube cannot distribute uniformly. Furthermore, from the test results of other specimens, the longitudinal strains distribute more unevenly along with the increase of global outward bulge, and more area of steel plate cannot reach yield.

As shown in Fig. (8), when reaching the maximum load, all the transverse strains have not reached yield. It reflects that the confinement effects on the core concrete at the peak load are small. However, it can be seen, in the post-peak stage, the transverse strains develop faster due to larger extrusion deformation of concrete. On the other hand, the global outward bulge of steel tube near the concave corner is so obvious that ε_{H1} of 7# and 9# develop faster than that of 5#, especially in the post-peak stage.

4. DESIGN METHODS

The methods for evaluating the maximum strength of axially loaded square or rectangular CFT columns are included in the existing design codes, such as the ACI [19], EC4 [20], GJB [21] and DBJ [22]. However, there is not any special method in design codes that can be used to evaluate the maximum strength of the cross-shaped CFT stub columns. The design methods in the existing codes can be optional methods to predict the strength of cross-shaped CFT stub column, but the application scopes should be smaller than the requested scopes in the codes. Therefore, at first, the application scopes of the maximum width-thickness ratio of steel plates and the strength of steel are discussed. Then, to establish a method with wider applicability, a theoretical method that adopts the superposition theory is proposed according to the experimental results in this paper. This proposed method practically considers the confinement effects of the cross-shaped steel tube on core concrete, together with the loss of longitudinal strength of steel tube caused by the outward bulge.

4.1. Application Scopes of the Design Methods in the Codes

Table 2 gives the comparison between the maximum strengths obtained by the methods in the codes and the experimental maximum loads (N_{uc}/N_u). As shown in Table 2, the experimental results of the specimens C1, C2 and C5 are obviously overestimated by the methods in the codes GJB and DBJ to at least 10%, while the evaluated strengths of the specimens C3 and C4 are relatively closer to the experimental results, especially for the specimen C3. The methods in the codes GJB and DBJ take into account the confinement effects of square or rectangle steel tube on the core concrete by applying magnification factors to the axial strength of the whole composite section. They require smaller limits of the width-thickness ratio of steel plate than those in other codes. For example, the $\alpha_1 \sqrt{f_{ys} / 235} / t$ should be smaller than 40 according to the code GJB, while it is equal to 52 in the code EC4. The purpose of stipulating smaller width-thickness ratio limit is to prevent large outward bulge or local buckling on the mid-span region of each steel plate in the square or rectangular CFT columns, so that more area of the steel tube can reach yield and the confinement effects on the core concrete are larger. Furthermore, the magnification factors considered in the code DBJ are larger than those in the code GJB.

Theoretically, for the cross-shaped CFT columns, if the confinement effects on the concrete and the stress distribution condition of steel tube are similar to those of square or rectangular CFT columns, the maximum strength can be evaluated by the codes GJB and DBJ. However, although the maximum width-thickness ratios of steel plates of all specimens ($\alpha_1 \sqrt{f_{ys} / 235} / t = 11 \sim 39$) do not exceed the limits that stipulated in the codes GJB and DBJ, but only the experimental results of the specimen C3 and C4, with the width-thickness ratios only 27% and 54% of the limit, respectively, are approximate to the predicted results. In fact, at the peak load, the global outward bulge of cross-shaped steel tube near the concave corners has key and significant effects on the stress distribution pattern of the steel tube and the confinement effects on the concrete, because in the test, the outward bulge or local buckling that occurred near the mid-span region of each steel plate was not obvious in the pre-peak stage. Under the transverse tensile stresses of the side- α_1 and side- b_1 steel plates, the concave corner of steel tube is subjected to an outward resultant force. So the edge intersected by the side- α_1 and side- b_1 steel plates can rotate and deform outward, and cannot be seen as a strict restrained boundary of the steel plates. The boundary conditions of the side- α_1 or side- b_1 steel plate are more like being

restrained elastically at the edge near the convex corner and being freedom at the edge near the concave corner. It is different from the boundary conditions of steel plates in a square or rectangular CFT column, which are restrained elastically at the both edges [24]. As a result, to restrict the global outward bulge at the concave corners and the local buckling in the mid-span of steel plates, the width-thickness ratio limit of the cross-shaped CFT columns should be smaller than that of the square or rectangular CFT columns, such as the case of the specimen C3.

Additionally, the adverse effects of outward bulge augment when the contribution of axial strength of steel tube to the bearing capacity is larger. For example, although the $\alpha_1 \sqrt{f_{ys} / 235} / t$ of the specimen C2 is smaller than that of the specimen C4, but its yield strength of steel is larger. Then the predicted results from the codes GJB and DBJ are unsafe for the specimen C2. Actually, for the specimen C4, although the differences between the N_{uc} and the N_u are less than 10%, but the maximum load in the experiment is somewhat overestimated, such as that the values of N_{uc}/N_u from the codes GJB and DBJ are 1.905 and 1.101, respectively. It is because that the thickness of steel plate of the specimen C4 is somewhat small. On the whole, for the cross-shaped CFT columns, conservatively, the methods in codes GJB and DBJ are suitable to evaluate the maximum strength of the columns with obvious confinement effects and with small loss of strength of steel tube caused by outward bulge, namely, with small width-thickness ratio of steel plate and small yield strength of steel, $f_{ys} \leq 261 \text{MPa}$ and $\alpha_1 \sqrt{f_{ys} / 235} / t \leq 11$, like the specimen C3.

The methods in the codes ACI and EC4 adopt the superposition method by simply combining the total yield strength of steel tube with the total axial strength of plain concrete. In fact, the theoretical value predicted by the method in code EC4 is nearly the same as the nominal strength (N_{un}), except that the cylinder axial compressive strength of concrete (f'_c) is adopted in the fomula of code EC4, $f'_c = 0.79 f_{cu,k}$. For the code ACI, an additional reduction coefficient 0.85 is adopted to decrease the strength of core concrete, so the calculated values are the smallest of the four codes. However, the strength reduction coefficient about core concrete cannot actually reflect the mechanical behaviour of cross-shaped CFT column. As shown in Table 2, both the standard deviation values of the N_{uc}/N_u , achieved from the codes ACI and EC4, are large. The method in code EC4 is suitable to evaluate the maximum strength of the columns without obvious confinement effects and with small loss of strength of steel tube, namely, with relative larger width-thickness ratio of steel plate than that of the specimen C3 and with small yield strength of steel, $f_{ys} \leq 239 \text{MPa}$ and $\alpha_1 \sqrt{f_{ys} / 235} / t \leq 22$, like the specimen C4. The method in code ACI, numerically, is suitable to evaluate the maximum strength of the columns without confinement effects and with large loss of strength of steel tube, namely, with relative large width-thickness ratio of steel plate and with large yield strength of steel, $f_{ys} \leq 348 \text{MPa}$ and $\alpha_1 \sqrt{f_{ys} / 235} / t \leq 27$, like the specimens C1 and C2. For the specimen C5, the yield strength of steel is large, $f_{ys} = 346 \text{MPa}$, and the width-thickness ratio of side- α_1 steel plate is the largest, $\alpha_1 \sqrt{f_{ys} / 235} / t = 39$, but it is still smaller than the limits required in the codes. However, the values of N_{uc}/N_u are 1.3~1.6, namely, its strength is significantly overestimated by all the methods in design codes.

Table 2. Comparison between the results obtained by the methods in the codes and the experimental results (N_{uc}/N_u).

No.	ACI[19]	EC4[20]	GJB[21]	DBJ[22]
C1	1.088	1.178	1.306	1.313
C2	1.016	1.079	1.132	1.241
C3	0.838	0.887	0.925	1.091
C4	0.876	0.961	1.095	1.101
C5	1.309	1.395	1.484	1.590
Mean value	1.025	1.100	1.188	1.267
Standard deviation	0.188	0.199	0.213	0.204

Notes: The strength of concrete adopted in the codes GJB and DBJ is $f_{ck} = 0.76 f_{cu,k}$, while that adopted in the codes ACI and EC4 is $f'_c = 0.79 f_{cu,k}$.

4.2. Proposed Method

By considering the confinement effects of the cross-shaped steel tube on the concrete, together with the loss of longitudinal strength of steel tube caused by outward bulge, a method for predicting the maximum strength of cross-shaped CFT columns with symmetrical section is proposed.

$$N_u = 4 \sum_{i=1}^2 \phi_{si} f_{ys} A_{si} + \phi_c f_{ck} A_c \tag{1}$$

where A_{si} and A_c are the area of each steel plate and the area of core concrete, respectively; ϕ_{si} is the strength reduction coefficient of each steel plate; i is the label of each steel plate, $i=1$ denotes the typical steel plates in a symmetrical cross-shaped section which are composed of the side- α_1 and side- b_1 steel plates, and $i=2$ denotes the other typical steel plates, such as the side- α_2 steel plate; ϕ_c is the strength magnification coefficient of core concrete used to consider the confinement effects.

The method raised by Ge [4] to calculate the value of ϕ_{si} of the square or rectangular CFT columns is used for reference. It is suitable for the side- a_2 steel plate directly. For the side- α_1 and side- b_1 steel plates, as discussed above, their boundary conditions are more like being restrained elastically at the edge near the convex corner and being freedom at the edge near the concave corner. So, it can be simply assumed that these two steel plates deform together as one steel plate, even there is an angle between them. According to Ge [4], when $R_i \leq 0.85$, local buckling will not occur before reaching the maximum load, then, where R_i is the coefficient about width-thickness ratio of each steel plate, calculated by

$$R_i = \frac{B_i}{t} \sqrt{\frac{12(1-\nu^2)}{4\pi^2}} \sqrt{\frac{f_{ys}}{E_s}} \tag{2}$$

where ν is the Poisson's ratio of steel; B_i is the width of each steel plate, especially, the side- α_1 and side- b_1 steel plates are assumed as one steel plate. When $R_i > 0.85$, the loss of longitudinal strength of steel tube due to outward bulge or local buckling should be considered. ϕ_{si} can be calculated by

$$\phi_{si} = \frac{1.2}{R_i} - \frac{0.3}{R_i^2} \leq 0.89 \tag{3}$$

ϕ_c is obtained by regression analysis method from the experimental data in this paper, and it is expressed by

$$\phi_c = 4.17 - 5.85\xi + 2.41\xi^2 \geq 1 \tag{4}$$

where $\xi = \frac{f_{ck} A_c}{f_{ys} A_s}$, it is called the confinement coefficient adopted in the code GJB.

As shown in Table 3, most of the experimental results are well predicted by the proposed method, except that of the specimen C5. The N_{uc}/N_u of the specimen C5 is equal to 1.153. It is somewhat overestimated, but it is already far more close to the experimental results than those predicted by the design codes. Conservatively, the proposed method can be adopted to accurately predict the maximum strength of the columns with $a_1 \sqrt{f_{ys} / 235} / t \leq 30$ and $f_{ys} \leq 345\text{MPa}$.

Table 3. Comparison between the results obtained by the new method and the experimental results (N_{uc}/N_u).

No.	C1	C2	C3	C4	C5	Mean value	Standard deviation
Results	1.100	1.018	0.981	1.028	1.153	1.056	0.069

CONCLUSION

The following conclusions can be drawn based on the results of this study.

1. The global outward bulge of steel tube near the concave corners of the cross-shaped CFT columns is significant at the peak load. It makes the stresses on the steel tube distribute unevenly, and the confinement effects on the concrete are inferior to the rectangular CFT columns. So the width-thickness ratio limit of steel plate should be smaller than that of the square or rectangular CFT columns.
2. With the decrease of width-thickness ratio of each steel plate, the global outward bulge near the concave corners was smaller, the confinement effects on the core concrete were increased, but the ductility could be improved only when it decreased by 2.08 times.
3. By increasing the yield strength of steel to 1.47 times, the bearing capacity and deformation at the peak load were inversely smaller, but the ductility was increased.
4. By increasing the length-width ratio of each leg of the cross-shaped section to 2.25 times, the global outward

bulge was increased and local buckling occurred earlier, the deformability became smaller.

5. Based on the experimental results in this paper, conservatively, the methods in codes GJB and DBJ can be adopted to evaluate the maximum strength of the cross-shaped CFT columns with $f_{ys} \leq 261 \text{ MPa}$ and $a_1 \sqrt{f_{ys} / 235} / t \leq 11$. The method in code EC4 can be adopted to evaluate the maximum strength of the columns with $f_{ys} \leq 239 \text{ MPa}$ and $a_1 \sqrt{f_{ys} / 235} / t \leq 22$. The method in code ACI can be adopted to evaluate the maximum strength of the columns with $f_{ys} \leq 346 \text{ MPa}$ and $a_1 \sqrt{f_{ys} / 235} / t \leq 27$.
6. The results predicted by the proposed method show better agreement with the experimental results than those provided by the design codes. Accurately, it can be adopted to predict the maximum strength of the columns with $a_1 \sqrt{f_{ys} / 235} / t \leq 30$ and $f_{ys} \leq 345 \text{ MPa}$.

CONFLICT OF INTEREST

The authors confirm that this article content has no conflict of interest.

ACKNOWLEDGEMENTS

This work was financially supported by the National Natural Sciences Foundation of China (No. 51408230, No. 51578246), the Fundamental Research Funds for the Central Universities (No. 2014ZM0015), the State Key Lab of Subtropical Building Science, South China University of Technology (No. 2013ZC14, No. 2013ZC20), Guangzhou Pearl River New Star of Science & Technology Project (No. 201610010077), and the Guangdong Provincial Natural Science Foundation of China (No. S2013040015140).

REFERENCES

- [1] C.W. Roeder, "Overview of hybrid and composite systems for seismic design in the United States", *Eng. Struct.*, vol. 20, no. 4-6, pp. 355-363, 1998.
[http://dx.doi.org/10.1016/S0141-0296(97)00035-7]
- [2] G.D. Hatzigeorgiou, "Numerical model for the behavior and capacity of circular CFT columns, Part I: Theory", *Eng. Struct.*, vol. 30, no. 6, pp. 1573-1578, 2008.
[http://dx.doi.org/10.1016/j.engstruct.2007.11.001]
- [3] J. Cai, and Z.Q. He, "Axial load behavior of square CFT stub column with binding bars", *J. Construct. Steel Res.*, vol. 62, no. 5, pp. 472-483, 2006.
[http://dx.doi.org/10.1016/j.jcsr.2005.09.010]
- [4] H.B. Ge, and T. Usami, "Strength analysis of concrete filled thin-walled steel box columns", *J. Construct. Steel Res.*, vol. 30, no. 3, pp. 259-281, 1994.
[http://dx.doi.org/10.1016/0143-974X(94)90003-5]
- [5] J. Cai, and Y.L. Long, "Axial load behavior of rectangular CFT stub columns with binding bars", *Adv. Struct. Eng.*, vol. 10, no. 5, pp. 551-565, 2007.
[http://dx.doi.org/10.1260/136943307782417663]
- [6] O. Yasuhiro, "An experimental study on axial and flexural behavior of concrete filled L-shaped steel tubes", *Archit. Inst. Jpn.*, vol. 8, pp. 1813-1814, 1992. [in Japanese].
- [7] Z.L. Zuo, J. Cai, X.Q. Zhao, C. Yang, and G. Sun, "Axial load behavior of L-shaped CFT stub columns with binding bars", *Eng. Struct.*, vol. 37, no. 4, pp. 88-98, 2012.
[http://dx.doi.org/10.1016/j.engstruct.2011.12.042]
- [8] Z.L. Zuo, J. Cai, C. Yang, and Q.J. Chen, "Eccentric load behavior of L-shaped CFT stub columns with binding bars", *J. Construct. Steel Res.*, vol. 72, no. 5, pp. 105-118, 2012.
[http://dx.doi.org/10.1016/j.jcsr.2011.11.003]
- [9] G.F. Du, L.H. Xu, and H.R. Xu, "Test study on behavior of T-shaped concrete filled steel tubular short columns under axial compression", *J. Huazhong Univ. Sci. Technol.*, vol. 25, no. 3, pp. 188-194, 2008. [Urban Science].
- [10] Z.L. Zuo, J. Cai, M.F. Liu, W.N. Duan, and Q.J. Chen, "Experimental study of T-shaped CFT stub columns with binding bars subjected to eccentric load", *J. Build. Struct.*, vol. 32, no. 8, pp. 79-89, 2011.
- [11] K. Uenaka, "Experimental study on concrete filled elliptical/oval steel tubular stub columns under compression Thin-Wall", *Structure*, vol. 78, pp. 131-137, 2014.
- [12] Y.S. Cao, H.N. Wang, and D. Wang, "The ductility of concrete-filled abnormality steel tube", *Ind. Constr.*, vol. 38, no. S1, pp. 473-475, 2008.
- [13] Z.H. Chen, Z.Y. Li, B. Rong, and X.L. Liu, "Experiment of axial compression bearing capacity for crisscross section special-shaped column composed of concrete-filled square steel tubes", *J. Tianjin Univ.*, vol. 39, no. 11, pp. 1275-1280, 2006.
- [14] Q.X. Ren, L.H. Han, D. Lam, and C. Hou, "Experiments on special-shaped CFST stub columns under axial compression", *J. Construct. Steel*

- Res., vol. 98, pp. 123-133, 2014.
[<http://dx.doi.org/10.1016/j.jcsr.2014.03.002>]
- [15] M. Yu, X.X. Zha, J.Q. Ye, and Y.T. Li, "A unified formulation for circle and polygon concrete-filled steel tube columns under axial compression", *Eng. Struct.*, vol. 49, pp. 1-10, 2013.
[<http://dx.doi.org/10.1016/j.engstruct.2012.10.018>]
- [16] B. Evirgen, A. Tuncan, and K. Taskin, "Structural behavior of concrete filled steel tubular sections (CFT/CFST) under axial compression", Thin-Wall", *Structure*, vol. 80, pp. 46-56, 2014.
- [17] Z.B. Chen, X. Chen, and Q.Y. Ye, "Structural design of Guangzhou New China Mansion", *J. Build. Struct.*, vol. 21, no. 3, pp. 2-9, 2000. [in Chinese].
- [18] Z. Tao, L.H. Han, and Z.B. Wang, "Experimental behaviour of stiffened concrete-filled thin-walled hollow steel structural (HSS) stub columns", *J. Construct. Steel Res.*, vol. 61, no. 7, pp. 962-983, 2005.
[<http://dx.doi.org/10.1016/j.jcsr.2004.12.003>]
- [19] ACI Committee 318, "*Building Code Requirements for Structural Concrete and Commentary*", Detroit (MI): 2005.
- [20] Eurocode 4 (EC4), *Design of Steel and Concrete Structures, Part 1. 1: General Rules and Rules for Building*. European Committee for Standardization: Brussels, 2004.
- [21] GJB 4142-2000, "*Technical Specifications for Early-strength Model Composite Structure used for Navy Port Emergency Repair in Wartime*", Chinese People's Liberation Army General Logistics Department: Beijing, 2001. (in Chinese)
- [22] DBJ13-51-2010, "*Technical Specification for Concrete-filled Steel Tubular*", Housing and Urban-Rural Development of Fujian: Fujian, 2003. (in Chinese)
- [23] B. Uy, "Local and post-local buckling of concrete filled steel welded box columns", *J. Construct. Steel Res.*, vol. 47, no. 8, pp. 47-72, 1998.
[[http://dx.doi.org/10.1016/S0143-974X\(98\)80102-8](http://dx.doi.org/10.1016/S0143-974X(98)80102-8)]
- [24] J. Cai, and Y.L. Long, "Local buckling of steel plates in rectangular CFT columns with binding bars", *J. Construct. Steel Res.*, vol. 65, no. 4, pp. 965-972, 2009.
[<http://dx.doi.org/10.1016/j.jcsr.2008.07.025>]

© Qiguang et al.; Licensee Bentham Open

This is an open access article licensed under the terms of the Creative Commons Attribution-Non-Commercial 4.0 International Public License (CC BY-NC 4.0) (<https://creativecommons.org/licenses/by-nc/4.0/legalcode>), which permits unrestricted, non-commercial use, distribution and reproduction in any medium, provided the work is properly cited.